Open Access Journal of Chemistry
Volume 2, Issue 3, 2018, PP 24-35
ISSN 2637-5834

Effect of Zinc Oxide Montmorillonite Composite the Removal of Arsenite

Davidson. E. Egirani[a], Nanfe. R. Poyi,[b] Napoleon Wessey[c]

[a]*Faculty of Science, Niger Delta University, Wilberforce Island, Nigeria.*
[b] *Nigerian Institute of Mining and Geosciences, Jos, Nigeria*
[c]*Faculty of Science, Niger Delta University, Wilberforce Island, Nigeria.*

***Corresponding Author:** Davidson. E. Egirani, Faculty of Science, Niger Delta University, Wilberforce Island, Nigeria.*

ABSTRACT

Here, the study was aimed at providing evidence that the presence of synthetic zinc oxide-montmorillonite composite, enhanced the adsorption of arsenite by ACOR montmorillonite. The batch mode systems were used to test the adsorption of arsenite on zinc oxide-ACOR montmorillonite composite. The experimental data involved the synthesis of zinc oxide-ACOR montmorillonite composite. The presence of zinc oxide coating on ACOR montmorillonite enhanced the adsorption of arsenite in aqueous solution. This was because the zinc oxide coating enhanced reorganization of active sites. The mechanism of the reaction indicated less than one proton coefficient of 0.51, < 1. The intraparticle diffusion with a slope of 13.90 (mgg-1) min0.5 and intercept 250.33, ≠ 0 was controlled by the boundary layer. The mass transfer rates were 1.654^-4 cm-2 hr-1, 5.593^-5 cm-2 hr-1 and 3.345^-5 cm-2 hr-1. There was an enhancement of mass transfer of adsorbate to the external layer of the adsorbent.

Keywords: *Activation; Adsorption; Clays; Colloids; Synthetic Methods; Kinetics*

INTRODUCTION

The aquatic environment is the biggest recipient of arsenic ions in both organic and inorganic forms. These inorganic forms namely arsenite and arsenate supersede other forms in the network [1][2]]. The presence of arsenic in drinking water constitutes a problem to humans and the ecosystem because it is toxic [3][4][5]. Carcinogens to humans are strongly linked to inorganic arsenic species [6][7][8].

Destruction of vital organs of the human body are indications of arsenic toxicity [9][10][11]. The bioaccumulation of arsenic leading to chronic health disorders has been reported [12] [13][14] [15][16][17].

Therefore, regulators of international and regional standards have reduced arsenic concentration in drinking water to 10 mgL^{-1} [18].

The hydrometallurgical treatment of chalcocite, covellite, and chalcopyrite to extract copper metal, generates slurries and leaching muds. These wastes contain a copper oxide, hydrated iron oxide, and impurities of lead, antimony, and germanium. In response to acid treatment, the pH of these slurries and leaching muds is usually less than 5. These wastes constitute modern sources of arsenite in groundwater. This is through infiltration into shallow wells [19][20]. These wastes are stored in sealed plastic tanks under reducing condition before discharge into the aquatic environment. This process stimulates the lowering of the concentration of metals and metalloid in the slurries and leaching mud [21][22]. The oxidation-reduction state of these metallurgical wastes has a substantial effect on the leaching of elements.

Under reducing condition, leached out metals and compounds including zinc oxide-montmorillonite interface will be negligible [23][24][25]. Therefore, there is a need to mimic in the laboratory, the removal of arsenite from hydrometallurgical contained-slurries.

Many factors control arsenic migration in the aquatic environment [26][12][13]. The adsorbent and chemistry of solutions control the active removal of dissolved arsenic species at low concentrations [27] [28].In addition, the hydrolysis of arsenic ions and species are residence time and solution pH-regulated

[1][29]. The diminution of arsenite removal from the aquatic environment is Cp-particle concentration, particle sizes and adsorbent chemistry regulated [30]. Aluminum coating on montmorillonite reduces adsorbate adsorption. The increase in arsenite removal as adsorbent particle concentration increases is linked to electrostatic coulombic interactions. However, increase in arsenite uptake as the solid concentration is increased does not occur all the time [13].

The surface area of adsorbent control arsenic uptake [31] [32]. Reorganization of mineral surfaces in aqueous solution is enhanced by residence time or aging [33]. The adsorption characteristic is taken as a simple technique for treatment of water when cost and design simplicity are considered [8][34]. The capacity of adsorption is dictated by an increase in arsenic concentration [33] [15].

The four steps of the mass transfer reaction mechanism have been linked to arsenite removal in aqueous solution: the film surrounding the adsorbent as the recipient of adsorbate, the surface of adsorbent as the recipient of adsorbate, intraparticle diffusion and adsorbent sites as the recipient of adsorbate. Here, the reaction mechanism is designated by Weber and Morris intraparticle diffusion model [35]. In aqueous solution, the fast process of intraparticle diffusion and slow process of electrostatic coulombic interactions are components of the reaction mechanism involved in arsenic uptake [36].

In addition, solution dilution and ion exchanges control the removal of arsenite from the aquatic environment [12][14]. Several workers [13] [37] [38] and others have reported the use of activated carbon and polyzwitterionic resin to remove metal ions from aqueous solution. The bare ACOR montmorillonite possesses the capacity to adsorb heavy metals using cation exchange and binds directly to the adsorbent surface via the aluminol and silanol sites [39][33].

Though several conservative methods have been used in the treatment of arsenic contaminated water [40][41] [42] [43] [44]], the use of zinc oxide nanoparticles supported by montmorillonite remains unclear. Some successive steps have been identified as ways for a solid-solution system migration. These include external mass transfer, intra-particle diffusion, protonation and adsorption of molecules of sorbate [45]. Therefore, models of reaction mechanism are necessary to determine the reactions involved.

Limited size water treatment systems demand the sourcing of innovative cost-effective treatment processes. Previously, the effect of bare ACOR montmorillonite on the removal of arsenite under similar experimental conditions have been studied [12][13]. Here, the study was aimed at providing evidence that the presence of synthetic zinc oxide-montmorillonite composite enhanced arsenite adsorption. This is in the treatment of arsenic contaminated water in relation to pH, residence time, arsenite initial concentration, the dosage of adsorbent and prolonged contact time. The ZnO- ACOR montmorillonite composite is a new novel adsorbent for arsenite removal. This has been applied in the treatment of arsenite in aqueous solution and is useful in the treatment of hydrometallurgical wastewater. This ZnO- ACOR montmorillonite composite significantly enhanced adsorption capacity of arsenite. The synthesis of the adsorbent and the testing of zinc oxide-ACOR montmorillonite composite to remove arsenite have been discussed.

EXPERIMENTAL

Materials and Reagents

Here, the analytical grade reagents were used. The montmorillonite was provided by Acros Organics company from Belgium. The ACOR montmorillonite used in this paper was washed with double distilled water. The Merck company from Germany provided the Arsenic (III) stock solution.

The AAS standard solution of 1000 mgL^{-1} arsenite was prepared from a titrisol ampule of arsenite in H_2O using a volumetric flask. As instructed by Merk guidelines, the content after filling up to mark was stored for use.

The working solutions of different concentrations were obtained by diluting the stock solutions. The precursor was zinc nitrate, and the precipitating agent was KOH. This was purchased from Sigma-Aldrich company in Belgium and used to synthesize zinc oxide nanoparticles.

Preparation of Anaerobic Suspensions

To create a reducing condition for all experimental content, all solutions were prepared using water that has been de-aerated and deionized. The deionized water was obtained from a Millipore Milli-Q system (18.2 MΩ.cm at room temperature). The experimental

content was bubbled through continuously for 24 hours using purified nitrogen gas. The content was securely sealed and stored in airtight containers in the anaerobic chamber in the dark before use [14].

Adsorbent Characterization

The ACOR montmorillonite and other adsorbents were verified by the X-ray diffraction (XRD) patterns of the product. pH of ACOR montmorillonite suspensions and reacting solutions were evaluated using the Model 3340 Jenway ion meter. The cation exchange capacity (CEC) was evaluated by Na saturation method. The determination of the specific surface area of the ACOR montmorillonite was conducted using the standard volumetric Brunauer, Emmett, and Teller (BET) method [46]. Here, the determination was by measuring the adsorption of the N_2 gas on the mineral solid phase at the boiling point of liquid nitrogen [47]. The determination of particle sizes of the adsorbent was done using coulter laser.

The spectral analysis was done using a JEOL JSM 5900 LV Scanning Electron Microscopy (SEM) with Oxford INCA Energy Dispersive Spectroscopy(EDS) [49]. The bare samples were viewed, and secondary electron images were acquired at low vacuum control pressure. The point of zero salt effect (PZSE) synonymous with the point of zero charges (pHzpc) of the ACOR montmorillonite was carried out using usual laboratory procedures [48][49]. The potentiometric titration was conducted after equilibration of 1% (by mass) of ACOR montmorillonite suspensions. 1:1 electrolyte solution initially adjusted to pH ranges near the PZSE were used as references.

Synthesis of Zinc Oxide Coated ACOR montmorillonite

The procedure was as reported elsewhere [50] and modified [51]. A solution of zinc nitrate ($Zn(NO_3)_2.6H_2O$) of 0.2 M concentration and KOH of 0.4M concentration were prepared with double distilled water. Here, 0.20 g of ACOR montmorillonite was mixed with 100 mL 1M $Zn(NO_3)_2$ solution and 180 mL of 2 M KOH solution. This was done to activate the ACOR montmorillonite. Subsequently, the KOH activated ACOR montmorillonite was dispersed into 150 mL of 0.2 M $Zn(NO_3)_2$ solution.

About 0.4 M KOH aqueous solution of three hundred microliters was titrated slowly at the rate of 1 mL/h. The content was subjected to vigorous stirring at ambient temperature. The stirring was done under nitrogen flow condition [52][2]. A double distilled water was used to wash the white precipitate. The white precipitate was centrifuged and finally washed with absolute alcohol. The washing was done to free the content from NO_3^- ions. Subsequently, the solid was heated at 450°C for 3 h in air. This process led to the formation of ZnO-ACOR montmorillonite composite.

Batch Mode Adsorption Experiments

To determine the effect of arsenite initial concentration, the suspension was made onto 50mL and subsequently equilibrated for 24h at pH=4. The As(III) solutions from10mgL^{-1} to 40mgL^{-1} have reacted with 1% each of ZnO-ACOR montmorillonite composite suspension. A range of solid concentrations of ZnO-ACOR montmorillonite composite from 2 gL^{-1} to 10 gL-1, made onto 50mL was reacted with solutions containing arsenite ions from10 mgL^{-1} to 40 mgL^{-1}. These solutions were equilibrated for 24h at pH=4.

These solutions were used to investigate the particle concentration effect (Cp). The arsenite concentrations from 10 mgL-1 to 40 mgL^{-1} was reacted with 1 % ACOR montmorillonite ZnO-ACOR montmorillonite composite at pH=4. The suspensions were made onto 50mL and aged from 24 - 720h. The aged suspension was used to investigate the effect of aging. The temperature at ambient condition was used to conduct all experiments in triplicates. To predict the reaction mechanisms, the proton coefficient otherwise known as the proton exchange isotherm was derived from the change of pH versus LogKd plot. This was based on the Freundlich isotherm [12][14] as given in equations (2, 3):

$$\propto SOH \leftrightarrow SO^- + \propto H^+ \quad (1)$$

$$logKd \leftrightarrow \log\left(K_p\{SOH\}^{\propto} + \propto pH\right) \quad (2)$$

Here, SOH equals the mineral surface-reactive site, SO- equals the surface-bound arsenite, log K_p equals the apparent equilibrium-binding constant and α equal the coefficient of protonation. The coefficient of protonation equals the number of protons displaced when one mole of arsenite binds to the mineral surface [12][53].

To determine this characteristic, 1% ZnO-ACOR montmorillonite composite suspension was regulated to the required pH, made into 50 mL, and reacted with arsenite ion solution of

10mgL-1. Secondly, the mass transfer rate and the intraparticle diffusion were derived from equations (3,4,5):

$$Q_t(mg/g)=[C_o-C_t]V/m \quad (3)$$

Here, Co equals the initial arsenite concentration (mgL-1) at time t=0, Ct equals the arsenite concentration (mgL-1) at time t, V equals the total ZnO-ACOR montmorillonite composite suspension volume and m is the weight of the adsorbent (g) [12][45]. The kinetics of arsenite ions adsorption to the mineral surface binding sites was controlled by the mass transfer constant K_f. Here, C_t/ C_o versus time provided the slopes of the curves derived from equation (4) [12]:

$$\left[\frac{d\left(C_t / C_0\right)}{dt}\right]_{t=0} \cong -K_f S_s \quad (4)$$

Here, C_0 and C_t denote the initial concentrations of arsenite and arsenite concentration at time t respectively, Ss equals the exposed specific surface area of ZnO-ACOR montmorillonite composite, and K_f equals the coefficient of mass transfer [54]. These models as reviewed previously [55] and derived from the Freundlich isotherm, were adopted to describe the adsorption of arsenite ions [45]. The Weber-Morris model was used to investigate the action of intra-particle diffusion on arsenite adsorption, [45] as given in equation (5):

$$Q_t = K_i t^{0:5} + C \quad (5)$$

Here, K_i equals the intraparticle diffusion constant (mgg^{-1} ^{min}) and the intercept (C) represents the effect of the layer boundary. K_i value was derived from the slope (K_i) of the plots of q_t versus $t0^{.5}$. A linear plot of q_t versus $t^{0.5}$ indicated that diffusion of intraparticle was involved in the process of adsorption.

For these reaction mechanisms, 1% ZnO-ACOR montmorillonite composite was reacted with $10mgL^{-1}$ arsenite ions solution. The content was made into 50mL and regulated to the required pH. The amounts of arsenite ions remaining in solution were determined after 2^{nd}h, 4^{th}h, 6^{th}h, 8^{th} h, 12^{th}h, 18^{th} h, and 24^{th} h.

At ambient temperature, these studies were done in triplicates and under the same experimental condition with those of bare montmorillonite. A 0.2 µm pore size cellulose acetate filter was used on the supernatant and content analyzed for arsenite ions, using a Hitachi Atomic Absorption Spectrophotometer (HG-AAS). The percentage of arsenite removed from solution was calculated from equation (6):

$$(\%)\text{of arsenite removed} = \left(\frac{C_0-C_e}{C_0}\right) x100 \quad (6)$$

where C_0 and C_e (mgL^{-1}) are the initial and equilibrium concentrations of the arsenite in solution.

RESULTS AND DISCUSSION

Results

In this study, the ACOR montmorillonite characterization has been provided (Table 1). The adsorbents involved in this study have been characterized and summarized (Table 1, Figs. 1-4). The X-ray diffraction spectrum indicated smectite as the key constituent. The EDS spectrum and SEM morphology indicated the presence of hydrous aluminosilicates. The point zero charge pHzpc was known as the point of zero salt effect was 7.13. This characteristic determines the positive and negative charge divide on the mineral surface. The external surface area of the adsorbent controls the quantity of exposed mineral surface available for reaction.

The proton coefficient (**(α)**) was based on a theoretical framework given by equations (1, 2), predicted and derived from the plot (Fig. 5), (Table 2). The value was 0.51. This pH plot had a maximum distribution coefficient (Kd) of $7.81mgg^{-1}$. The intraparticle diffusion was based on a theoretical framework given by equation (5), predicted and derived from the plot (Fig. 6), (Table 3). The intraparticle diffusion constant derived from the slope was 13.90 (mg^{-1}) $min^{0.5}$ and the intercept C was 250.33, ≠ 0. This plot consisted of three linear parts with the first part representing the external mass transfer. The second and third part represented the intraparticle diffusion and adsorption inside the adsorbent surface. Here, the maximum adsorption capacity was $731mgg^{-1}$ at the 24^{th} h. The mass transfer constants (K_f) predicted from equations (3, 4) and derived. from Fig. 7 are given (Tables 4). Also, this characteristic consisted of three linear parts. The second linear part started after the 4^{th} h and the third linear part started after the 8^{th} h. Fig. 8 had a statistical slope of 77.51 and intercept of $22.00mgg^{-1}$ (Table 5). There was an increase in the capacity of adsorption as arsenite initial concentration increased. The maximum adsorption capacity of 3000 mgg^{-1} occurred at $40mgL^{-1}$. Fig. 9 consisted of a complex plot over the range of Cp investigated. There was a linear decrease in the

capacity of adsorption as particle concentration increased. The highest adsorption capacity was 3052 mgg^{-1} at 2 gL^{-1}.

The adsorption capacity increased with an increase in residence time (Fig. 10). The linear fit adsorption pattern aimed at mimicking the adsorption pattern (Table 6) revealed an intercept 721.26 (mgg^{-1}) and a slope of 0.18. The adsorption capacity increased from 730mgg^{-1} to 860 mgg^{-1} over the range of residence time investigated. The maximum adsorption capacity was 860 mg/g at the 720th h. The adsorption capacity generally increased with an increase in contact time (Fig. 11). Predicted from equation 6, the rate of removal of arsenite ions increased from 69% to 86% over the range of contact time investigated.

Table1. *Characteristics of ACOR montmorillonite*

Characteristics	Weight %
SiO_2	54.00±0.03
Al_2O_3	17.00±0.05
Fe_2O_3	5.20±.01
CaO	1.50±0.04
MgO	2.50±0.05
Na_2O	0.40±.01
K_2O	1.50±0.05
Moisture content	9.30±0.05
Loss on Ignition	15.00± 0.024
CEC (mmols/g)	56.00±0.01
% (<1000 nm) colloid	0.53±0.03
Particle size range (μm)	0.01-80.00±0.04
pH± σ	2.00±0.05
Surface Area(SSA±σ) (m^2/g)	10.00± 0.024
Point of Zero Salt Effect (PZSE)	7.13±0.04

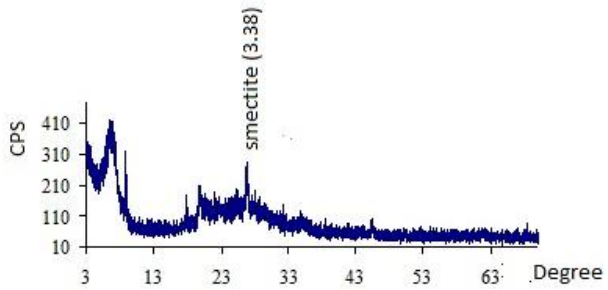

Fig1. *X-ray diffraction of montmorillonite*

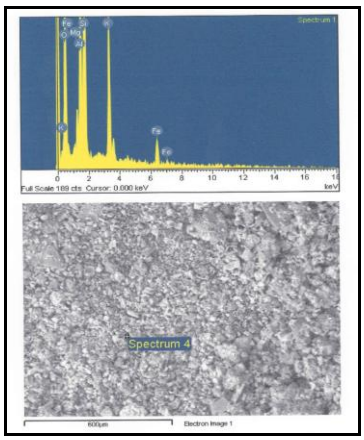

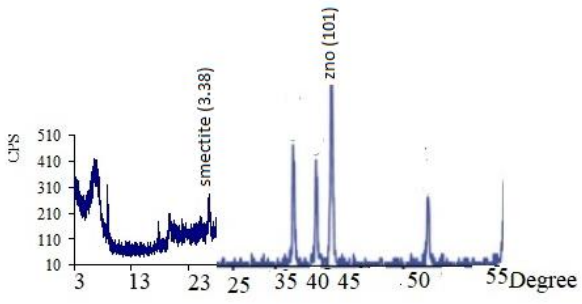

Fig2a. *EDS /SEM for ACOR montmorillonite showing element peaks and particle sizes.*

Fig2b. *X-ray diffraction of synthetic zinc oxide -montmorillonite showing peaks*

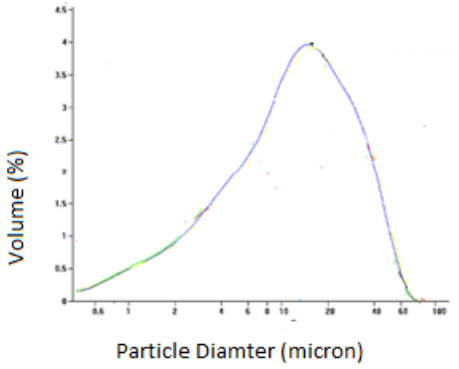

Fig3. *Particle size distribution of ACOR montmorillonite at suspension pH*

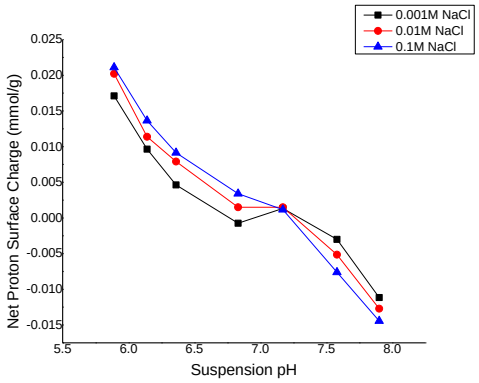

Fig4. *Plot of net proton charge versus suspension pH*

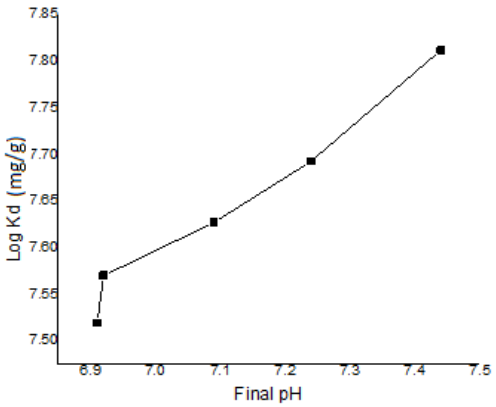

Fig5. *Plot of Log Kd (distribution coefficient) versus final pH for proton coefficient*

Table2. *Statistical presentation of proton coefficient derived from Fig. 5*

Equation	**Y=a+b*x**		
Proton coefficient α	0.51		
Log Kd(mgg^{-1})		**Value**	**Standard Error**
	Intercept	3.98	$8.14^{\wedge-6}$
	Slope	0.51	$1.14^{\wedge-6}$

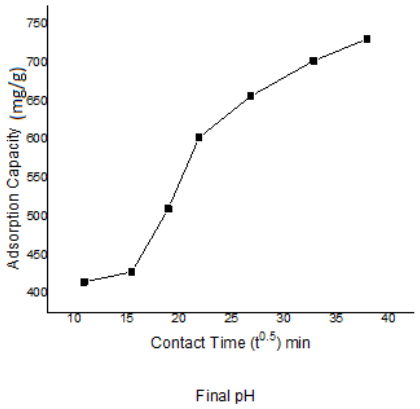

Fig6. *Plot of Adsorption capacity versus time for intraparticle diffusion*

Table3. *Statistical presentation of intraparticle diffusion data derived from linear fit of Fig. 6*

Equation	Y=a+b*x		
		Value	**Standard Error**
$Q_t(mgg^{-1})$ $min^{0.5}$	Intercept	250.33	0.00
	Slope	13.90	$1.73^{\wedge-4}$

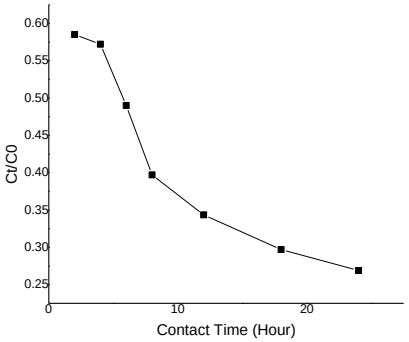

Fig7. *Plot of Ct/Co versus contact time for mass transfer rates*

Table4. *Mass transfer rates for As(III) adsorbed on ZnOcoated montmorillonite derived from Fig. 7*

Slope I (hr^{-1})	**SlopeII (hr^{-1})**	**SlopeIII (hr^{-1})**	**Exposed Surface Area (cm^2)**	**K_{fI} ($cm^{-2}hr^{-1}$)**	**K_{fII} ($cm^{-2}hr^{-1}$)**	**K_{fIII} ($cm^{-2}hr^{-1}$)**
0.165	0.055	0.033	1000	$1.654^{\wedge-4}$	$5.593^{\wedge-5}$	$3.345^{\wedge-5}$

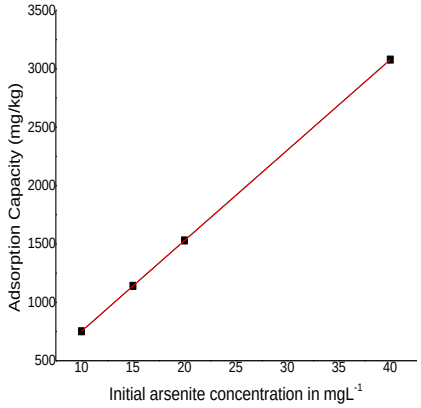

Fig8. *Plot of adsorption capacity versus initial arsenite concentration at pH=4 and solid concentration =2 gL^{-1}*

Table5. *Linear fit for Fig. 8*

Equation	y = a + b*x		
Adsorption Capacity (mg/g)	Intercept	Value	Standard Error
		22.00	0.04
Adsorption Capacity	Slope	77.51	0.00

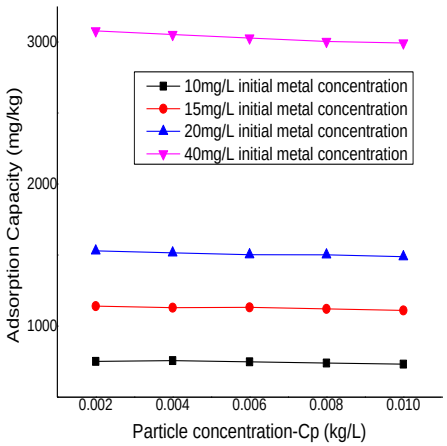

Fig9. *Plot of sorption capacity versus Cp at pH=4 for particle concentration effect*

Table6. *Linear fit for Fig. 10*

Equation	y = a + b*x		
Adsorption Capacity (mg/g)	Intercept	Value	Standard Error
		721.26	0.00
Adsorption Capacity	Slope	0.18	4.93^-6

Reaction Mechanism

The reaction mechanism was discussed based on the proton coefficient, the intraparticle diffusion and the mass transfer rates. In previous studies devoid of coated zinc oxide, proton coefficient α was 1.13 [12][13][14].

Here, α for ZnO-ACOR montmorillonite composite was 0.51. This value was slightly less than the value recorded in previous studies (Table 2). This characteristic suggested that protonation was controlled and attenuated by the ZnO-ACOR montmorillonite composite. This characteristic was an indication that protonation was lowered in the presence of zinc oxide coating.

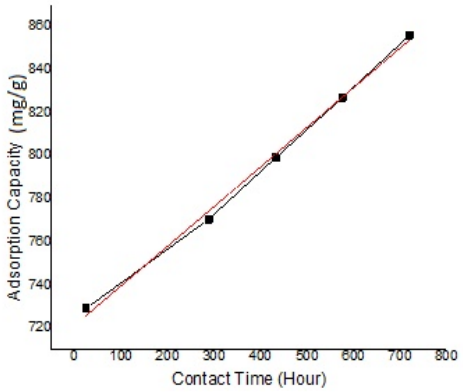

Fig10. *Plot of adsorption capacity versus residence time –ageing for mineral systems at pH=4 and 10mgL^{-1} arsenite concentration*

The presence of this coating could mask the acidic sites on the edges and planar surfaces of ACOR montmorillonite. The three steps of mass transfer have been recognized in the reaction mechanism of arsenite with ZnO-montmorillonite composite.

These features include, film diffusion, adsorbent surface diffusion and intraparticle diffusion. (Figs. 6-7; Tables 3-4). Though Intraparticle diffusion was involved in the adsorption process (Fig. 6 and Table 3), this was not a rate-limiting reaction.

Also, there was indication of boundary layer control. In comparison with previous studies [13][14], the slope and intercept for the bare ACOR montmorillonite were higher than those of the ZnO-ACOR montmorillonite composite, thus suggesting that the presence of zinc oxide coating attenuated intraparticle diffusion.

When compared with previous studies, the mass transfer rates for the bare ACOR montmorillonite were higher than results for the ZnO-ACOR montmorillonite composite [14], thus suggesting the enhancement of mass transfer of arsenite to the external layer of the ZnO- ACOR montmorillonite composite (Fig. 7).

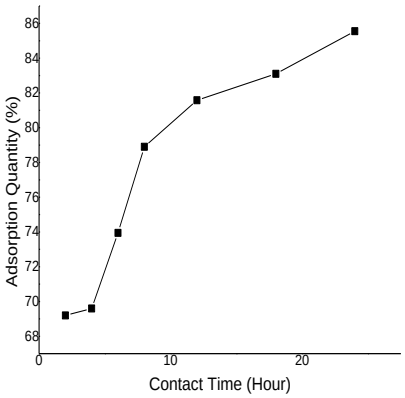

Fig11. *Plot of adsorption capacity versus time at 10mgL^{-1} arsenite concentration*

Reaction kinetics

The arsenite adsorption depended on contact time. This was derived from the plot of adsorption capacity versus time (Fig. 6, Fig. 11). The assessment was from 2 to 24h at ambient temperature and initial arsenite concentration of 10 mgL^{-1} at pH= 4. In this reaction, the adsorption capacity increased with increase in contact time and began to plateau at the 12th h. Thus, there was evidence of gradual saturation of adsorption sites. This agreed with earlier reports [12][45]. These two reports were for arsenite adsorbed on bare ACOR montmorillonite and organically modified montmorillonite respectively. The adsorption rate was initially fast and the capacity of adsorption increased over time. This agreed with an earlier report [28].

The initial quick adsorption of arsenite in the first phase may be related to larger numbers of active adsorption sites [12][56].

The investigation of different arsenite concentrations was necessary since contaminated aquatic systems present different concentrations of arsenic. Here, the increase in adsorption capacity as arsenite concentration was increased suggested that the mass transfer rate of arsenic ions between the solid-solution divide was not controlled by a concentration gradient (Fig. 8). This was different from cases reported elsewhere [57][14]. In both cases, there was a reported decrease in adsorption capacity for some heavy metals reacted with montmorillonite (100 to 300mgL^{-1}). In this report, the constant linear plot indicated a unified increase in capacity of adsorption due to non-saturation of the active and reactive sites. The complex decreases in adsorption over the range of Cp investigated were different from an earlier report [13], for arsenite adsorbed on bare ACOR montmorillonite.

There, an increase in the concentration of particle led to increasing adsorption capacity. Here, the changes in the adsorption pattern were higher at different arsenite concentration (Fig. 9). This characteristic suggested that the presence of zinc oxide coatings led to the strengthening of linkages between adsorbate and adsorbent concentrations as the reaction proceeded.

Again, an increase in Cp suggestively led to low pressure at the solid-solution interface, decrease in surface area, reactive sites, and concentration gradient effect. Thus, there was a decrease in arsenite diffusion to reactive sites. In this report, an increase in adsorption capacity as aging was increased, depicted a linear increase rather than a complex decrease in adsorption pattern (Fig. 10). This adsorption pattern was different from a case reported elsewhere [13] for arsenite adsorbed on bare ACOR montmorillonite over the same range of ageing. Previously, it has been reported that a complex decrease in adsorption pattern existed. This characteristic was linked to intra-particle diffusion, essentially controlled by inner-sphere complexation [13]. In this report, the linear increase in adsorption pattern was essentially controlled by outer-sphere water molecule bonding, hydrolysis and reactive support of zinc oxide coating. Thus, this led to an increased reorganization of active sites.

As the solution pH was increased protonation and hydroxylation of a mineral surface controlled the adsorption process (Fig. 5). This adsorption process was different from a previous report [13] in the absence of ZnO coating. In that case, there was a complex increase in adsorption as pH was increased outside the point of zero charges.

Here, surface charges on the ZnO-ACOR montmorillonite surface affected the role of solution pH. The point of zero charges (pHzpc)

of ACOR montmorillonite was approximately 7.13. As the pH was increased around the point of zero charge, there was a decrease in protonation and enhancement of hydroxylation. This process favored arsenite adsorption. In addition, the stability of zinc oxide is in the pH range of more than 7, and as reported elsewhere [58], the optimum adsorption of arsenite was expected above pH 7.

CONCLUSIONS

The presence of ZnO-ACOR montmorillonite composite enhanced the reorganization of active sites and arsenite adsorption. Here, the synthesis of ZnO-ACOR montmorillonite composite was done, and characterization conducted using usual laboratory techniques.

The batch mode systems were used to test the adsorption of arsenite on ZnO-ACOR montmorillonite composite. The mechanism of the reaction was tested. These tests included proton coefficient that was less than one, an intraparticle diffusion that was controlled by the boundary layer and mass transfer rates that were lower than those of bare ACOR montmorillonite.

There was a linear increase in adsorption capacity as arsenite concentration was increased, thus indicating that the active and reactive sites of the ZnO-ACOR montmorillonite composite were not yet saturated. The complex characteristics of adsorption over the range of Cp investigated, suggested the following: (i) decrease in surface area, (ii) reactive sites and (iii) concentration gradient effect. The decrease in adsorption capacity in this situation, suggested an increase in particle size and aggregation of the mineral system as the reaction proceeded.

The adsorption of arsenite was increased by aging. The maximum adsorption of arsenite was 860 mgg^{-1} over the range of residence time investigated.

The higher magnitude of adsorption pattern was essentially controlled by hydrolysis and reactive support of zinc oxide coating including increased reorganization of active sites.

As the pH was increased, deprotonation and hydroxylation of ZnO-ACOR montmorillonite composite controlled the adsorption process.

As the contact time was increased, there was a decrease in protonation and enhancement in hydroxylation, thus leading to an adsorption increase of arsenite. Here, the adsorption of arsenite increased from 69% to 86% over the range of contact time investigated.

These results supported the need to source different nano-sized coatings to treat toxic materials in the environment. In comparison with other findings by [57][12], ZnO-ACOR montmorillonite composite significantly enhanced the adsorption of arsenite in aqueous solution. Here, future work would be on the testing removal of toxic materials using other coated clay minerals.

ACKNOWLEDGEMENTS

The authors remain grateful to the Niger Delta University for the usual research allowances provided for the running of research projects.

CONFLICT OF INTEREST

Authors have no conflict of interest to declare.

REFERENCES

[1] Ghorbanzadeh N, Jung WH, Kabra AN, Jeon B.-H. Removal of arsenate and arsenite from aqueous solution by adsorption on clay minerals. Geosystem Engineering. (2015; 18 302-311.

[2] Wang D, Lin Z, Wang T, Yao Z, Qina M, Zhengd S, Lu W. Where does the toxicity of metal oxide nanoparticles come from: The nanoparticles, the ions, or a combination of both?, Journal of Hazardous Material. 2016; 308:328–334.

[3] Fauser P, Sanderson H, Hedegaard RV, Bossi R, Larsen JB. Occurrence and sorption properties of arsenicals in marine sediments, Environ. Monitor. and Assessment. (2013;185: 4679-4691.

[4] Cao Y, Guo Q, Shu Z, Zhao Q, Ren T Application of calcined iowaite in arsenic removal from aqueous solution, Applied Clay Science, 2016; 126: 313-321.

[5] Aktar S, Jahan M, Alam S, Hossain K, Saud ZA. Individual and combined effects of Arsenic and Lead on behavioral and biochemical changes in mice, Biological Trace Element Research. 2017; 177:288-296.

[6] Jinamoni S, Goswami S, Archana S. Arsenic removal from water by adsorption utilizing natural kaolinite clay of Assam, Research J. Chemistry and Environ. 2011; 15:559-563.

[7] Zhang M, Gao B, Varnoosfaderani S, Hebard A, Yao Y, Inyang M. Preparation and characterization of a novel magnetic biochar for arsenic removal, Environmental Science. 2011;23: 1947–1954.

[8] Nahar N, Rahman A, Ghosh S, Nawani N, Mandal A. Functional study of $AtACR_2$ gene putatively involved in accumulation, reduction

and/or sequestration of arsenic species in plants, Biologia (Poland). 2017; 72: 520-526.

[9] Na P, Jia X, Yuan B, Chen Y, Wang L. Arsenic adsorption on Ti-pillared montmorillonite, Journal of Chemical Technology and Biotechnology. 2010; 85:708-714.

[10] Jain CK, Ali I Arsenic: Occurrence, toxicity and speciation techniques, Water Research. 2000; 34: 4304–4312.

[11] Boddu VM, Abburi K, Talbott JL, Smith ED, Haasch R. Removal of As(III) and As(V) from aqueous medium using chitosan-coated biosorbent, Water Research. 2008; 42:633–642.

[12] Egirani DE, Andrews JE, Baker AR. Arsenite removal from aqueous solution by mixed mineral systems I. Reactivity and removal kinetics. Inter. Recent Scientific Res. 2013a; 4: 357-363.

[13] Egirani DE, Andrews JE, Baker AR. Arsenite removal from aqueous solution by mixed mineral systems ii, The role of solution composition and ageing, Inter. Recent Scientific Research. 2013b; 4:439- 443.

[14] Egirani DE, Andrews JE, Baker AR. Arsenite removal from aqueous solution using mixed mineral systems injected with zinc sulfide under sulfidic- anoxic condition i: reactivity and removal kinetics, J. Environmental Sci., Computer Sci. and Eng. & Technology. 2014a; 3:893-910.

[15] Egirani DE, Andrews JE, Baker AR. Arsenic removal from aqueous solution using mixed mineral systems injected with sphalerite under sulfidic- anoxic conditions ii, The Role of Solution Composition and Ageing, J. Environmental Science., Computer Sci. and Eng. & Technology. 2014b; 3:881-892.

[16] Egirani DE, Wessey N, Aderogba A. Effect of mineral systems injected with zinc sulfide on arsenite removal from aqueous solution: part ii, American J. Applied Chemistry. 2015; 3: 201-206.

[17] Egirani DE, Wessey N. Effect of clay and goethite mineral systems inoculated with pyrite on arsenite removal from aqueous solution., Chemical Technol. & Metallurgy. 2016; 51 735-746.

[18] WHO (World Health Organization). Guidelines for Drinking Water, In: Misstear B, Banks D, Clark L (eds) Water wells and boreholes. E-Publication, John Wiley & Sons 2017; pp. 467-472

[19] Kuncoro EP, Isnadina DRM, Darmokoesoemo H, Fauziah OR, Kusuma HS. Characterization, kinetic, and isotherm data for adsorption of $Pb^{2+}$from aqueous solution by adsorbent from mixture of bagasse-bentonite, Data In Brief. 2018; 16:622-629.

[20] Zhang Y, Cao B, Zhao L, Sun, L, Gao Y, Li J, Yang F. Biochar-supported reduced graphene oxide composite for adsorption and co-adsorption of atrazine and lead ions, Applied Surface Science. 427:147–155.

[21] Plescia P, Maccari D. Recovering metals from red mud by thermal treatment and magnetic separation'. Journal of Minerals, Metals, and Materials Society. 1996; 48:25-28.

[22] Tavares FO, Pinto LADM, Bassetti FDJ, Bergamasco R, Vieira AMS. Environmentally friendly biosorbents (husks, pods and seeds) from Moringa oleifera for Pb(II) removal from contaminated water, Environmental Technology. 2017; 38:3145-3155.

[23] van der Sloot HA. Systematic leaching behavior of trace elements from construction materials and waste material, Studies in Environmental Sci.1991; 48:19-36.

[24] Romero M, Rincón JM. Surface and Bulk Crystallization of Glass-Ceramic in the Na_2O-CaO-ZnO-PbO-Fe_2O_3-Al_2O_3-SiO_2 System Derived from a Goethite Waste'. Journal of American Ceramic Soc. 1999; 82:1313-1317.

[25] Jha MK, Kumar VJ Singh R. Review of hydrometallurgical recovery of zinc from industrial wastes, Resources, Conservation and Recycling. 2001; 33:1-22.

[26] Khezami L, Taha KK, Modwi A. Kinetic and thermodynamic studies of trivalent arsenic removal by indium-doped zinc oxide nanopowder, Digest J. Nanomaterials and Biostructures. 2016; 11:1397-1410.

[27] Awual M, REl-Safty SA, Jyo A. Removal of trace arsenic and phosphate from water by a highly selective ligand exchange adsorbent, Spectrochimica Acta Part A. 2013; 100:161–165.

[28] Ren X, Zhang Z, Luo H, Yang C, Li L. Adsorption of arsenic on modified montmorillonite, Applied Clay Science. 2014; 97-98:17-23.

[29] Mohan D, Pittman Jr. CU. Arsenic removal from water/wastewater using adsorbents—A critical review, J. Hazard Material. 2007; 142:1-53.

[30] Waeles M, Vandenhecke J, Salaun P, Cabon J, Riso RD. External sources vs internal processes: What control inorganic arsenic speciation and concentrations in the Penze estuary, Journal of Marine Systems. 2013; 109–110: 261–272.

[31] Sahmoune MN. The role of biosorbents in the removal of arsenic from water, Chemical Engineering and Technology. 2016; 39: 1617-1628.

[32] Anjum A, Lokeswari P, Kaur M, Datta M. Removal of As (III) from aqueous solutions using montmorillonite, J. Analytical Sci., Methods and Instrumentation. 2011; 1:25-30.

[33] Luo X, Liu H, Huang G. Remediation of arsenic-contaminated groundwater using media-injected permeable reactive barriers with a modified montmorillonite: sand tank studies, Environ. Sci. Pollution Research. 2016; 23:870.

[34] Moussawi RN, Patra D. Modification of nanostructured ZnO surfaces with curcumin: fluorescence-based sensing for arsenic and improving arsenic removal by ZnO, Royal Soc. Chem. Advance. 2016; 6:17256-17268.

[35] Alswata AA, Ahmad MB, Al-Hada NM, Kamari HM, Hussein MZB, Ibrahim NA. Preparation of Zeolite/Zinc Oxide Nanocomposites for toxic metals removal from water, Results in Physics. 2017; 7: 723-731.

[36] Gray PJ, Tanabe CK, Ebeler SE, Nelson JA. Fast and fit-for-purpose arsenic speciation method for wine and rice, J. Anal. Atomic Spectrometry. 2017; 32:1031-1034.

[37] Omer OS, Hussein BHM, Hussein MA, Mgaidi A. Mixture of illite-kaolinite for efficient water purification: Removal of As(III) from aqueous solutions, Desalination and Water Treatment. 2017; 79:273-281.

[38] Saleh TA, Rachman IB. Ali SS Tailoring hydrophobic branch in polyzwitterionic resin for simultaneous capturing of Hg(II) and methylene blue with response surface optimization. Chemical Engineering J. 2017a; 307:230-238.

[39] Saleh TA, Seri A. Tuzen M Optimization of parameters with experimental design for the adsorption of mercury using polyethyleneimines modified-activated carbon, Journal of Environmental and Chemical Engineering. 2017b; 5:1079-1088.

[40] Jain A, Agarwal M. Kinetic equilibrium and thermodynamic study of arsenic removal from water using alumina supported iron nano particles, J. Water Process Engineering. 2017; 19: 51-59.

[41] Li D, Guo X, Tian Q, Xu R, Zhang L Synthesis and application of Friedel's salt in arsenic removal from caustic solution, Chemical Engineering J. 2017; 323:04-11.

[42] Gogoi P, Adhikari P, Maji TK. Bioremediation of arsenic from water with citric acid cross-linked water hyacinth (E. crassipes) root powder, Environ. Monitor. and Assessment. 2017; 189: 383.

[43] Guo X, Jin X, Zhao X, Zhang J, Qiu N. Nano-adsorptive effects manifested in arsenite adsorption onto the nano-sized goethite, Sci. Advanced Mater. 2014; 6: 793-802.

[44] Wang W, Yan L, Duan J, Jing C. Arsenite adsorption removal from acid wastewater using titanium dioxide adsorption filter column, Chinese J. Environmental Engineering. 2017; 11:1322-1328.

[45] Bandpei AM, Mohseni SM, Sheikhmohammadi A, Nazari S, Rezaei S. Optimization of arsenite removal by adsorption onto organically modified montmorillonite clay: Experimental & theoretical approaches, Korean J. Chemical Eng. 2017; 34:376-383.

[46] Brunauer S, Emmett PH, Teller E. Adsorption of gases in multimolecular layers, J. Am. Chem. Society. 1938; 60:309–319.

[47] Lowell S, Shields JE. Powder surface area and porosity, Springer, Netherlands, 1991.

[48] Nazir MS, Kassim MH, Mohapatra L, Gilani MA, Raza MR, Majeed K. Characteristic properties of nanoclays and characterization of nanoparticulates and nanocomposites, In Jawaid M, Qaiss A, Bouhfid R. (eds) Nanoclay Reinforced Polymer Composites. Engineering Materials, E-Publication, Springer, 2016.

[49] Tournassat C, Davis JA, Chiaberge C, Grangeon S, Bour IC the acid–base properties of montmorillonite edge surfaces. Environ. Sci. Technology. 2016; 50:13436–13445.

[50] Egirani DE, Latif MT, Poyi NR, Wessey N, Acharjee S. Synthesis and characterization of kaolinite coated with cu-oxide and its effect on the removal of aqueous mercury(ii) ions: part ii, Int. Res. J. Chemistry and Chemical Science. 2017; 4:043-048.

[51] Ghorbani HR, Mehr FP, Pazoki H, Rahmani BM. Synthesis of ZnO nanoparticles by precipitation method, Orient. Journal of Chemistry. 2015; 31: 1219-1221.

[52] Maruthupandy M, Zuo Y, Chen J-S, Song J-M, Niu H-L, Mao C-J, Zhang S-Y, Shen Y-H. Synthesis of metal oxide nanoparticles (CuO and ZnO NPs) via biological template and their optical sensor applications: The key laboratory of environment friendly, Applied Surf. Science. 2017; 397:167–174.

[53] Jia Z, Wang Q, Zhu C, Yang G. Adsorption of ions at the interface of clay minerals and aqueous solutions, INTECH, Croatia, 2016.

[54] Shi Z-J, Guo Q, Xu Y-Q, Wu D, Liao S-M, Zhang F-Y, Zhang Z-Z, Jin R-C. Mass transfer characteristics, rheological behavior and fractal dimension of anammox granules: The roles of upflow velocity and temperature, Bioresource Technology. 2017; 244:117–124.

[55] Qiu H, Lu LV, Bing-cai PAN, Qing-jian Z, Wei-ming Z, Quan-xing Z. Critical review in adsorption kinetic models, Journal of Zhejiang University Science A. 2009; 10:716-724.

[56] Zhang J, Ding T, Zhang C. Biosorption and toxicity responses to arsenite in Scenedesmus quadricauda, Chemosphere. 2013; 92:1077-1084.

[57] Akpomie KG, Dawodu FA, Adebowale KO. Mechanism on the sorption of heavy metals from binary-solution by a low-cost

montmorillonite and its desorption potential, Alexandria Eng. J. 2015; 54:757-767.

[58] Samad A, Furukawa M, Katsumata H, Suzuki T, Kaneco S. Photocatalytic oxidation and simultaneous removal of arsenite with CuO/ZnO photocatalyst, J. Photochemistry and Photobiology A Chem.2016; 325:97–103.

Citation: *Davidson. E. Egirani, Nanfe. R. Poyi, Napoleon Wessey .(2018). "Development Effect of Zinc Oxide Montmorillonite Composite the Removal of Arsenite". Open Access Journal of Chemistry, 2(3), pp.24-35.*